(Received 23 February 2025, Accepted 10 September 2025, Scheduled 22 September 2025)

Effect of Electron Beam Irradiation on Differently Treated Carbon Fiber-Filled Acrylonitrile Butadiene Styrene for EMI Shielding

Adel M. Alkaseh[1, 3], Mohd Edeerozey Abd Manaf[1], Zurina Shamsudin[1], Mohammed Iqbal Shueb[2], Mohammed Yousif Zeain[4], Bilal Salman Taha[5, 6], Muhammad Inam Abbasi[4, *], and Adam Wong Yoon Khang[4]

[1] *Faculty of Industrial and Manufacturing Technology and Engineering, Universiti Teknikal Malaysia Melaka Hang Tuah Jaya, 76100 Durian Tunggal, Melaka, Malaysia*
[2] *Radiation Processing Technology Division, Malaysian Nuclear Agency Bangi, 43000, Kajang, Selangor, Malaysia*
[3] *Polymer Research Centre, Tripoli, Libya*
[4] *Centre for Telecommunication Research & Innovation (CeTRI) Faculty of Engineering and Technology Electronics and Computer (FTKEK) Universiti Teknikal Malaysia Melaka (UTeM), Melaka 76100, Malaysia*
[5] *Department of Electrical and Electronics Engineering, University Tenaga Nasional, Malaysia*
[6] *Institute of Microengineering and Nanoelectronics (IMEN), Universiti Kebangsaan Malaysia (UKM), Malaysia*

ABSTRACT: The burgeoning reliance on electronic devices in sectors such as aerospace systems and consumer electronics necessitates robust electromagnetic interference (EMI) shielding. Current challenges often involve balancing material performance with sustainability and cost-effectiveness. This study addresses these needs by exploring the use of recycled carbon fiber (rCF) in acrylonitrile butadiene styrene (ABS) composites for enhanced EMI shielding, contributing to more sustainable material development. We investigated the impact of different rCF treatments (untreated, chemically treated, and chemically-mechanically treated) on mechanical properties (tensile strength, stiffness, flexibility) and EMI shielding effectiveness of these composites. Furthermore, the role of electron beam (EB) irradiation at 200 kGy in creating cross-linked structures to boost conductivity and shielding performance was thoroughly examined. Fabricated via melt compounding, the composites' electrical conductivity, and EMI shielding capabilities were the main focus. Results show that the EB-irradiated composite with 30 wt% chemically treated rCF achieved a peak electrical conductivity of 1.34×10^{-8} S/m and an impressive shielding effectiveness of 46.13 dB. These findings offer crucial insights for developing high-performance, cost-efficient, and potentially sustainable rCF-filled ABS composites for advanced EMI shielding applications.

1. INTRODUCTION

Electromagnetic interference (EMI) refers to the disturbance caused by the transmission of electromagnetic energy from one electronic device to another that affects an electrical circuit by electromagnetic induction, electrostatic coupling or conduction [1, 2]. This undesired EMI effect can cause a malfunction in electronic systems, disruption of communication, as well as affecting human health [3]. As electrical and electronic devices are becoming an integral part of our daily life, shielding for EMI is needed and is increasingly required by governments around the world. EMI shielding uses metals as well as magnetic materials to simultaneously suppress or lessen the electric and magnetic fields. The purpose is to isolate electromagnetic waves and hence, effectively contain the radiation of electromagnetic waves from one area to another [4, 5].

Previously, metal and alloy shrouds had been used to avoid EMI-induced functional disruption in electrical and electronic devices. However, they were unable to meet the requirements of lightweight, flexible, and miniaturized instruments due to their disadvantages such as high density, high cost, and low efficiency [6, 7, 50]. With the increase in demand for low-cost and lighter electronic devices, studies on plastics as EMI shielding materials have gained attention. To enable plastics to be used as shielding materials, their electrical conductivity needs to be enhanced. This can be achieved through two general approaches, i.e., coating with conductive metal and blending with conductive fibers or particles [8, 9, 53]. However, coating has disadvantages such as delamination added with a requirement for additional surface preparation and special equipment, which eventually increases the cost of final products [10].

The blending technique is an effective method for fabricating conducting polymer composites by incorporating conductive fillers into the polymer matrix. Unfortunately, some conductive fillers such as metal powders and carbon black are not suitable as EMI shielding material due to high filler loading requirements for such applications, as much as 40 to 60

* Corresponding author: Muhammad Inam Abbasi (inamabbasi@utem.edu.my).

wt% [11]. In addition, several studies have reported the use of carbon nanotubes (CNTs) as fillers at low volume fractions to produce effective EMI shielding material [12–13]; however, their high cost makes this approach undesirable. The use of carbon blacks improved mechanical properties as well as EMI shielding effectiveness (SE) but was required in very high volumes [14]. On the other hand, carbon fibre (rCF) is a filler that is effective for the enhancement of electrical conductivity in polymer composite at low filler content [13, 15]. Metasurfaces, including frequency-selective surfaces (FSSs), are revolutionizing electromagnetic wave control for communication and security. A notable example is the use of a chirality-assisted metasurface [50] to encode holographic images through a full-polarimetric synthetization scheme, enabling highly secure information encryption. FSS has also been applied to manipulate electromagnetic waves for advanced technologies [51], such as enhancing the performance of 5G communication systems. Building on this, article [52] introduces the concept of non-orthogonal metasurfaces to achieve a nearly 100% transmission efficiency for arbitrary polarization transformations, which is crucial for efficient communication and multiplexing.

The final mechanical properties of carbon fibre reinforced polymer (CFRP) composites are determined not only by the intrinsic properties of the reinforcing CFs and polymer matrices but also by the interface that connects these two components. CF surfaces are chemically inert, resulting in weak interfacial bonds between the CFs and matrix, preventing the achievement of optimal mechanical properties [16, 17]. Several CF surface treatment methods, including wet chemical or electrochemical oxidation [18, 19], polymer or metal coating [20, 21], and plasma treatment [22, 23], have been proposed to improve the interfacial adhesion between CFs and the surrounding polymer matrix. Grafting nanostructures, such as nanotubes and nanoparticles, onto the surface of CFs is a popular method for improving the interface properties of CF composites [24-26]. The grafting process can be carried out using a simple dip-coating method [27], chemical grafting [28], chemical vapor deposition (CVD) [29, 30], or electrophoretic deposition (EPD) [17]. However, many of these treatments have drawbacks and limitations.

Achieving enhanced conductive stability in polymer composites is critical for reliable EMI shielding. While chemical crosslinking often faces limitations due to high-temperature requirements, radiation crosslinking, particularly electron beam (EB) irradiation, offers an advantageous ambient-temperature alternative. Previous research has established that EB irradiation can notably improve the electrical consistency and mechanical performance of various conductive polymer composites, including acrylonitrile butadiene styrene [16, 17]. Building upon this, the present study comprehensively investigates the synergistic effects of electron beam irradiation and varied carbon fiber treatments on the mechanical properties, electrical conductivity, and EMI shielding effectiveness of ABS/recycled carbon fiber (rCF) composites. Our primary objective is to scientifically delineate how different rCF surface modifications — untreated, chemically treated, and chemically-mechanically treated — influence composite performance before and after EB irradiation at a specific dose of 200 kGy. The methodological framework involves systematic material preparation via melt compounding, followed by detailed characterization of mechanical performance (tensile strength, stiffness, and flexibility), electrical conductivity, and EMI shielding effectiveness across a relevant frequency range. Through this experimental scope and sequence, this research aims to advance current knowledge by providing a deeper understanding of tailored ABS/rCF composites for high-performance EMI shielding, particularly highlighting the role of sustainable rCF and electron beam processing in enhancing composite reliability and shielding efficiency in demanding applications.

2. MATERIAL AND METHODS

2.1. Materials

The matrix material used in this study was acrylonitrile butadiene styrene (ABS), which possesses numerous versatile applications, including aircraft interiors, electronic housing, and automotive moldings and dashboards. The commercial acrylonitrile butadiene styrene resin (HI-121H) was acquired from LG Industries in Korea. ABS was employed in the composites in the form of pelletized material.

The matrix material used in this study was acrylonitrile butadiene styrene (ABS), which possesses numerous versatile applications, including aircraft interiors, electronic housing, and automotive moldings and dashboards. The commercial acrylonitrile butadiene styrene resin (HI-121H) was acquired from LG Industries in Korea. ABS was employed in the composites in the form of pelletized material. Waste carbon fiber prepregs were used as the source of recycled carbon fibers (rCF) and supplied by a Malaysian composite company. The prepregs were made of carbon fibre-reinforced epoxy resin. The waste carbon fiber, presented as sheet fiber, was used in three forms: as-received CF prepreg, chemically treated CF, and chemically mechanically treated CF. The specific type of the waste carbon fiber is not reported because of a confidential agreement. The chemicals used to treat recycled carbon fibers were nitric acid (68%) and ethanol (95%). The nitric acid used for the removal of resin from CFRP and the ethanol used for cleaning waste carbon fibre from impurities residue were provided by Polyscientific Enterprise Sdn. Bhd.

2.2. Treatment of rCF

They were used in three forms, i.e., as-received CF prepreg, chemically treated CF, and chemically mechanically treated CF. The as-received carbon fibers (rCFs) prepregs were initially cut into smaller sizes measuring 3 mm before the fiber treatment. The cut prepregs underwent chemical and mechanical treatments to extract CFs which were used as reinforcement in ABS. They were treated with nitric acid (68%) at a temperature of 115°C to remove any resins present on the surface. This treatment lasted for 40 minutes. To reach the desired pH level equivalent to that of distilled water (pH = 5.5–6), the fibers were rinsed with distilled water for thirty minutes. Following this, the samples were immersed in ethanol (95%) for one hour using an ultrasonic cleaner. The recycled carbon fibers (rCFs) were then dried at a temperature of 60°C for twenty-four

hours to eliminate moisture before compounding. Before the mechanical modification of recycled carbon fiber, the chemically treated carbon fibers were dried in an oven. Subsequently, the fibers were pulverized using pulverize into smaller sizes measuring at 90 µm. Following the pulverization process, they were filtered using a sieve-shaker machine to ensure uniform fiber size. The rCF was crushed to reduce its size, allowing for the formation of composite samples through melt mixing and hot compression processes. Subsequently, all recycled carbon fibres (treated and untreated) were added to ABS polymer to fabricate composite samples using melt mixing and hot compression moulding techniques.

2.3. Composite Fabrication

Initially, a dry mixing of acrylonitrile butadiene styrene (ABS) and recycled carbon fibre (rCF) was performed using a high-speed mixer at room temperature for five minutes, before melting compounding. The amount of rCF was varied at 5, 10, 15, 20 25, and 30 wt%. Next, the compounds of ABS and rCF were mixed by using the mixer, then were extruded by a single screw extruder. Subsequently, the fabricated composite samples were exposed to EB produced with three MeV acceleration voltages and 10 mA beam current. The irradiation dose used at each pass was 200 kGy.

2.4. Testing and Analysis

Tensile properties were determined for each composition using a testing machine with a fixed cross-speed of 5.00 mm/min and a load range of -20 to 100 N. Six specimens were tested at each cross-head speed and constant temperature, and the average values were recorded. The scanning electron microscopy (SEM) model ZEISS EVO 50 was employed to examine the cross-section surfaces of the samples at magnifications of 200x, 1000x, and 3000x. X-ray diffraction (XRD) analysis was performed using an X-ray diffractometer (PANalytical, X'Pert Pro MRD) with nickel-filtered copper Kα radiation at $\lambda = 0.154$ nm. The electrical resistivity of ABS/rCF was determined from the resistance values obtained using an LCR meter (Agilent, E4980A). Electrical conductivity, σ, is then taken as the reciprocal of resistivity. EB irradiation (NHV EPS-3000) was used to develop EB irradiation-induced rCF reinforced ABS composites. All samples of ABS/rCF composites were exposed to electron beam (EB) irradiation at 200 kGy doses to assess the effects of EB radiation on the properties of the composites. Figure 1 shows a clear schematic diagram of the EMI shielding effectiveness measurement setup.

2.5. EMI Shielding Effectiveness Measurement

Electromagnetic interference (EMI) shielding effectiveness (SE) is a critical parameter used to evaluate how well a material or enclosure can block or attenuate electromagnetic interference. Measuring EMI shielding effectiveness involves a series of standardized procedures, typically performed in controlled laboratory environments using specialized equipment. Signal generators and analyzers (such as network analyzers) are used to generate and measure electromagnetic signals at specific

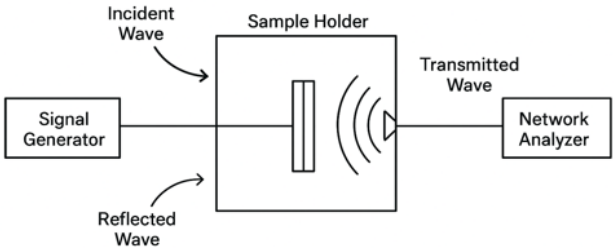

FIGURE 1. EMI shielding effectiveness measurement.

frequencies. Figure 1 shows a schematic diagram of EMI shielding effectiveness measurement setup.

An EMI shielding effectiveness measurement setup typically involves a vector network analyzer (VNA), antennas, and a shielded enclosure, often an anechoic chamber, to assess how well a material or structure blocks electromagnetic interference. The core of the measurement is to compare the signal strength received with and without the shield in place, quantifying the shielding effectiveness in decibels (dB). The VNA is the central instrument. It generates a signal that is transmitted by one antenna and received by another. It measures the amplitude and phase of both the incident and transmitted/received signals. VNA analyzes the S-parameters (scattering parameters) to determine the shielding effectiveness. Appropriate antennas are chosen based on the frequency range of interest and the type of electromagnetic field being measured. Typically, transmitting and receiving antennas are used to create a signal path through or around the shielding material. A shielded enclosure, often an anechoic chamber, is used to minimize external interference and reflections, ensuring accurate measurements. Figure 2 shows illustration of the EMI shielding effectiveness measurement setup.

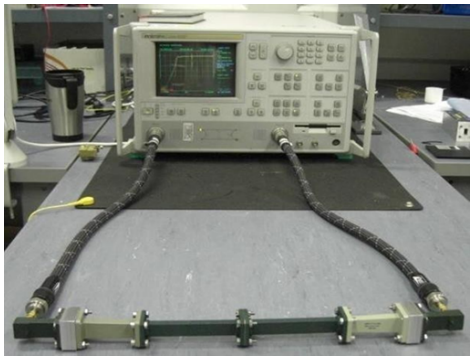

FIGURE 2. Illustration of the EMI shielding effectiveness measurement setup.

3. RESULTS AND DISCUSSION

3.1. Mechanical Properties

Figures 3, 4, and 5 detail the mechanical properties of the rCF/ABS composites, including tensile strength, elongation at break, and Young's modulus. Figure 3 demonstrates that adding recycled carbon fiber generally enhances the composites' tensile strength, with a peak observed at 30 wt%. For instance,

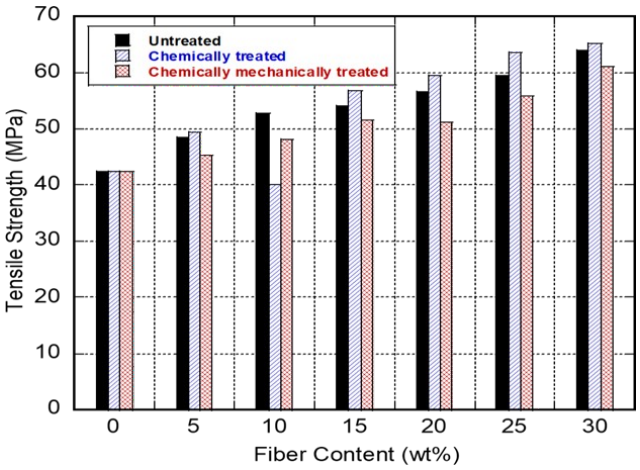

FIGURE 3. Average tensile strength of rCF/ABS composites.

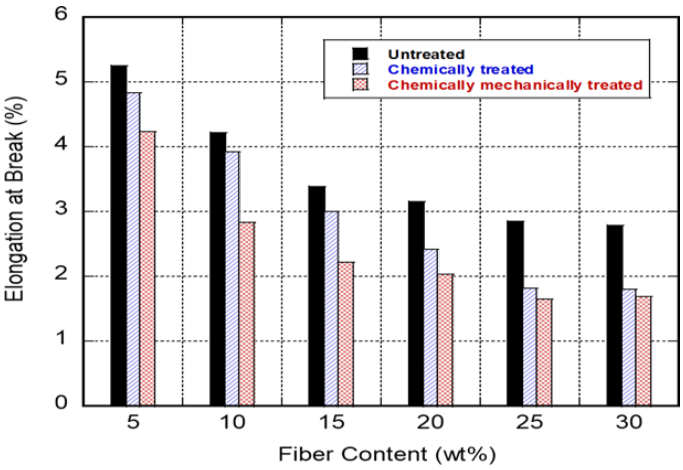

FIGURE 4. Average elongation at break of rCF/ABS composites.

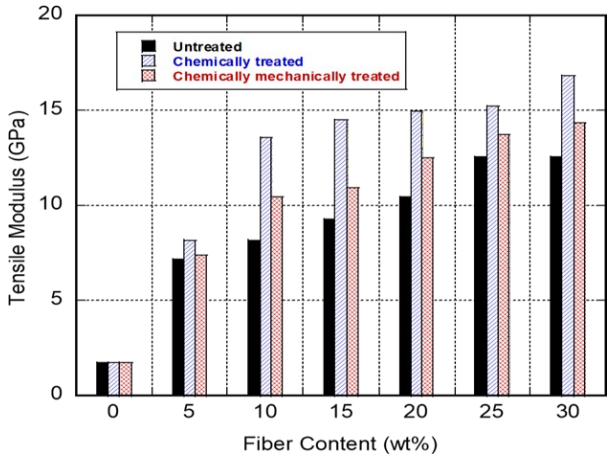

FIGURE 5. Average of Young's modulus of rCF/ABS composites.

at this loading, untreated, chemically treated, and chemically-mechanically treated rCF/ABS composites showed significant strength increases of 61.12, 63.95, and 65.24 N/mm^2, respectively. It is noteworthy that chemically-mechanically treated rCF consistently yielded higher tensile strengths than pure ABS, highlighting the importance of surface treatment in improving fiber-matrix adhesion and, consequently, load transfer [31]. While increasing rCF content generally improved tensile strength, an observed decrease at 10 wt% for chemically treated rCF was attributed to potential fiber damage from excessive oxidation, suggesting an optimal treatment balance.

The observation that strength peaks at 30 wt% rCF is consistent with the typical behavior of filled polymer composites. Initially, as rCF content increases from lower percentages (e.g., 5% to 30%), the fibers act as reinforcing agents, effectively sharing and transferring load within the polymer matrix. This leads to a progressive increase in mechanical properties like tensile strength and stiffness. However, beyond a certain filler concentration (in our case, 30 wt%), further increasing the rCF content would likely lead to a reduction in strength. This phenomenon is primarily due to the agglomeration of carbon fibers. At higher loadings, rCF particles tend to clump together due to increased fiber-fiber interactions, leading to poor dispersion within the ABS matrix. These agglomerates act as stress concentration points and defects, reducing the effective load transfer between the fibers and polymer, thus compromising the overall mechanical integrity of the composite. Additionally, higher filler content can decrease the relative amount of polymer available to effectively bind and wet out all the fiber surfaces, further weakening the composite.

The determination of 30 wt% as optimal was based on a systematic experimental approach. We prepared and characterized composites across a range of rCF loadings (e.g., 5%, 15%, 30%, and potentially higher percentages in preliminary or unreported trials). Mechanical testing (e.g., tensile tests, as referenced implicitly by "strength") was performed for each composition. The peak observed at 30 wt% indicates the highest mechanical performance achieved within our studied range. While we did not present data for rCF content beyond 30 wt% in Figure 3 (to maintain focus on the optimal range for the presented data), the theoretical understanding of composite behavior strongly suggests that further increases would lead to diminishing returns or even degradation of mechanical properties due to the aforementioned agglomeration effects. Therefore, based on empirical data from comprehensive testing within the explored range and established composite mechanics principles, 30 wt% was identified as the optimal loading for maximum strength.

Even though the lowest tensile strength was observed in untreated rCF at all weights, it is noticeable that tensile strength improved when untreated rCF content increased. For chemically treated rCF, it has been found that the rCF content gradually improves the tensile strength. However, the tensile strength at 10 wt% has decreased, likely due to the damage to carbon fibres from excessive oxidation. Therefore, it can be concluded that the chemically treated rCF content is more effective in increasing tensile strength than untreated rCF, as demonstrated by the significant increase in tensile strength in chemically mechanically treated rCF/ABS composites. This treatment resulted in a higher tensile strength than pure ABS.

It is widely recognized that surface treatment of carbon fibers is essential for improving the adherence of the fibers to the polymer matrix and, as a result, enhancing the mechanical properties of the composites. Furthermore, the tensile strength of three

TABLE 1. Average values of tensile strength of rCF/ABS composites.

Name	Tensile Strength (MPa)		
Composites	Chemically-Mechanically CF/ABS	Chemically Treated CF/ABS	Untreated CF/ABS
0%	42.5	42.5	42.5
5%	48.52	49.33	45.23
10%	52.73	39.54	48.12
15%	54.08	56.73	51.53
20%	56.55	59.47	51.15
25%	59.56	63.52	55.74
30%	63.95	65.24	61.12

TABLE 2. Average of elongation at break of rCF/ABS composites.

Composites	Elongation at Break (%)		
	Untreated CF/ABS	Chemically Treated CF/ABS	Chemically-Mechanically Treated CF/ABS
0%	10.45	10.45	10.45
5%	5.25	4.84	4.23
Composites	Elongation at Break (%)		
10%	4.21	3.92	2.84
15%	3.39	3.01	2.22
20%	3.15	2.41	2.03
25%	2.86	1.82	1.65
30%	2.78	1.81	1.69

types of composites increases with increasing fiber loading, except for chemically treated CF at 10 wt%, which falls below the value of pure ABS.

These results support a study by [33], which stated that increasing short carbon fiber (SCF) content in the ABS as a matrix improves tensile strength by efficiently removing the epoxy size through HNO3 treatment and enhancing the interfacial adhesion of ABS/rCF composites [31]. Therefore, these findings provide evidence supporting the hypothesis that the presence of rCFs improves the tensile strength of the entire composite. Table 1 shows the average tensile strength of rCF/ABS Composites.

The elongation at break refers to the material's ability to withstand changes in shape without cracking. Figure 4 illustrates the average elongation at break for rCF/ABS composites. Overall, the addition of carbon fiber reduced the percentage of elongation compared to pure ABS. The untreated CF/ABS composite with a 5 wt% carbon fiber loading exhibited the highest elongation at break at 5.25%. Conversely, the elongation at break generally decreased with rCF addition compared to pure ABS, as is typical for reinforced brittle polymers. However, chemically-mechanically treated rCF at 30 wt% (1.69%) showed the lowest elongation, while untreated rCF at 5 wt% (5.25%) had the highest. This indicates that while stiffness increased, the material became less ductile. This result suggests that the toughness increased with chemically-mechanically treated CF, thereby improving the composites' ability to absorb energy in the plastic region due to the finer fiber structure that promotes fibre-matrix interaction. This mechanism prevents cracks between the fiber and matrix, leading to increased interfacial bonding. Consequently, the composite demonstrated higher elongation at break with chemically mechanically treated CF. Table 2 presents the average elongation at break for rCF/ABS composites.

Figure 5 displays the measurements of Young's modulus for all the samples. Young's modulus refers to the stiffness of a material in the elastic range of a tensile test. The graph in Figure 5 demonstrates the influence of fibre content on the average Young's modulus of rCF/ABS composites as a function of the rCF weight fraction (wt%). According to the graph, Young's modulus of ABS increases as more rCF is added. For example, Young's modulus increases from 1.7 GPa for pure ABS to 12.58, 16.83, and 14.36 GPa for untreated rCF/ABS, chemically treated rCF/ABS, and chemically-mechanically treated rCF/ABS composites, respectively. These findings align with the research conducted by [33], which also observed that an increase in short carbon fiber (SCF) content in the ABS matrix improved Young's modulus due to enhanced adhesion at the ABS/rCF composite interface [31]. Additionally, the ABS-chemically treated rCF composite demonstrates improved properties compared to the untreated rCF composite, thanks to better fibre/resin compatibility. Notably, a 10% loading of chemically mechanically treated rCF provides the same elastic modulus as a 20% loading of untreated rCF, and a 10% loading of chemically treated rCF provides the same elastic modulus as a 30% loading of untreated rCF. These results are consistent

TABLE 3. Average of Young's modulus of rCF/ABS composites.

Name	Tensile Modulus GPa		
Fiber Content	Untreated CF/ABS	Chemically Treated CF/ABS	Chemically-Mechanically TreatedCF/ABS
0%	1.7	1.7	1.7
5%	7.19	8.15	7.41
10%	8.2	13.58	10.45
15%	9.26	14.48	10.96
20%	10.45	14.93	12.53
25%	12.55	15.22	13.74
30%	12.58	16.83	14.36

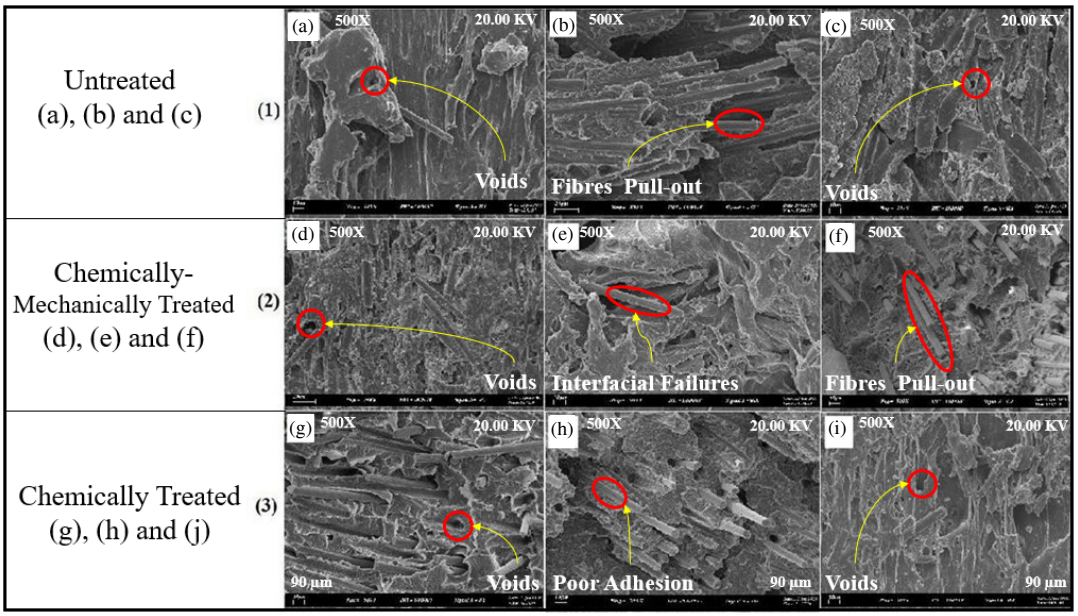

FIGURE 6. (a)–(j): SEM images for irradiated rCF/ABS Composite (500X mag): [1: Untreated: (a) 5% rCF/95% ABS, (b) 15% rCF/85% ABS, and (c) 30% rCF/70% ABS Composite. 2: Chemically- Mechanically Treated: (d) 5% rCF/95% ABS, (e) 15% rCF/85% ABS, and (f) 30% rCF/70% ABS. 3: Chemically Treated: (g) 5% rCF/95% ABS, (h) 15% rCF/85% ABS, and (j) 30%rCF/70% ABS.

with the findings of [32], which observed that both ultimate tensile stress and Young's modulus increased with increasing recycled carbon fibre loading in polyethene composites [33]. Table 3 shows the average Young's modulus of the rCF/ABS composites.

3.2. Morphological Analysis

In Figure 6, SEM images show the surface morphology of the samples of 5, 15, and 30 wt% of irradiated rCF/ABS composites with 500X magnification. After irradiation, 5, 15, 30 wt% of irradiated rCF dispersed in rCF/ABS composite showed changes in surface morphology. It was found that after irradiation, the polymeric structure suffered significant damage, which was also responsible for the decrease in crystallinity of the material. The SEM images display that there has been an improvement in the interfacial adhesion between rCF and the polymer matrix in the irradiated samples. A morphology study has shown that interfacial adhesion increases with higher irradiation doses [32]. The exposure of polymers or polymer blends to high-energy radiation at room temperature is a relatively new method that can be employed to modify their properties by altering the molecular structure of polymers or enhancing blend compatibility [32]. A noticeable difference in fracture morphology can be observed when the specimen is compared with the irradiation to the one without. The fibre surfaces seem strong and are surrounded by a layer of polymer. These findings suggest that good adhesion has been achieved, and the morphology of the composites noticeably differs from those without irradiation. According to the research findings, it seems that electron beam radiation processing has a positive effect on interfacial adhesion in ABS/rCF composites. This can be attributed to the formation of radiation-induced grafting and crosslinking. This phenomenon appears to contribute to enhancing the overall performance of the material.

The fracture surface micrographs of thermally conductive ABS/rCF composites, both unirradiated and EB-irradiated, suggest that there has been an improvement in the compat-

ibility between different components. This improvement is likely a result of the grafting and crosslinking reactions that occur due to EB irradiation. EB irradiation causes the creation of free radicals in ABS, which subsequently triggers diverse chemical reactions at the interface of the thermally conductive ABS/rCF composites. These reactions include rearrangement, branching, and crosslinking. Additionally, EB irradiation may also result in the formation of non-covalent interactions, including hydrogen bonds. The interaction between the matrix ABS and the dispersed thermally conductive fillers, rCF, is effectively enhanced by the combination of the covalently bonded micro-crosslinked network structure and the non-covalent hydrogen bond interaction.

The SEM images reveal microstructural differences in differently treated recycled carbon fiber (rCF)/ABS composites. These treatments affect fiber morphology and surface characteristics. For untreated rCF/ABS composites, the fiber surface is smooth to lightly smoothened due to original sizing. This results in minimal surface roughness, with common observations of gaps, weak interfacial bonding, and low interfacial adhesion. Larger voids or debonded regions may be present under load due to poor adhesion. For chemically treated rCF/ABS composites, the SEM images show reduced void content at the interface, more intimate contact with reduced gaps, and evidence of better wet-out around fibers. For chemically mechanically treated rCF/ABS composites, clear evidence of chemical bonding zones adjacent to physically rough regions with the presence of a transitional interphase is demonstrated. The wet-out with the ABS was highly improved, with the matrix surrounding the fibers more uniformly, even in roughened regions.

The chemically treated case, which is synonymous with the EB-irradiated samples, demonstrates superior results compared to the other two. This is evidenced by significant improvements in interfacial adhesion, as seen in the SEM (see Figures 6(a)–(j)), and a more robust fracture morphology. The positive outcomes are attributed to the formation of both covalent bonds, through radiation-induced grafting and crosslinking, and non-covalent hydrogen bonds. This combined bonding mechanism effectively enhances the compatibility between the ABS matrix and rCF fillers, resulting in a material with noticeably better overall performance than the untreated and chemically-mechanically treated composites.

3.3. The XRD Analysis

An X-ray diffraction (XRD) test at room temperature was conducted in this section to confirm the variations in the crystallinity of ABS and its composites with differently treated recycled carbon fiber (rCF). XRD spectra, as shown in Figures 7(a) and (b), of 5% rCF/95% ABS composite and 30% rCF/70% ABS composite revealed the amorphous nature of both composites. The XRD spectra of rCF and irradiated rCF composites in the figures show that after irradiation, the interlayer spacing of rCF increased, and a small decrease in the interlayer spacing range was visible. This could be attributed to changes in functional groups. The other two bands appear at 36.65° and 77.15° for treated 5% rCF and 95% ABS, respectively, and 43.7° and 58.11° for treated 30% rCF and 70% ABS,

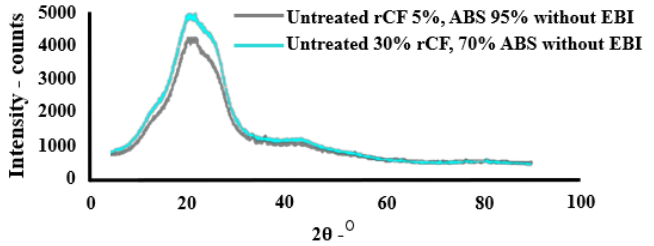

FIGURE 7. XRD of non-irradiated ABS/rCFs, (a) rCF 5%, ABS 95%, (b) 30% rCF, 70% ABS.

which correspond to the limited ordering in the few layers of rCF and disordered carbon materials. It is worth noting that, after irradiation, these two bands exhibit almost no change [34].

From Figure 7(a), the XRD pattern of the 5% rCF/95% ABS composite exhibited a diffractive peak centered at $2\theta = 19.8°$, indicating that the composite is in an amorphous state because ABS has no true melting point. Both the samples containing 5% rCF/95% ABS and 30% rCF/70% ABS showed broad halos with a peak at approximately $2\theta = 19.8°$ and no signs of crystallinity peaks, indicating their amorphous nature.

Upon comparing Figures 7(a) and (b), it can be observed that as the concentration of recycled carbon fiber increased, the intensity of the peaks also increased, irrespective of whether it was a broad diffraction peak. It is easily found that there is a broad peak at 20.40; this peak was caused by the oxidation of carbon fiber [35].

Figures 8(a) and (b) illustrate the XRD curves of rCF/ABS blends when they are exposed to an irradiation dosage of 200 kGy. In Figure 8(a), there is an appearance of a significant and broad single peak centered at $2\theta = 20.4°$ for the irradiated 5% rCF/95% ABS sample. The peak broadening impact has resulted in a decrease in crystallinity [36]. However, the peak gradually broadens as the percentage of ABS increases.

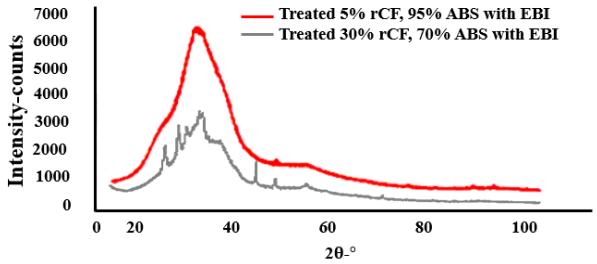

FIGURE 8. X-Ray diffraction of irradiated ABS/rCFs composites, (a) treated rCF 5%, ABS 95%, (b) treated 30% rCF, 70% ABS.

In other words, the spectra indicate that composites only display the dispersion peak of ABS at 10°–30°. The shape and intensity of this dispersion peak in thermally conductive ABS/rCF composites mostly stay the same under EB irradiation. This is because the changes caused by EB radiation primarily take place in the amorphous region, resulting in the products remaining in their amorphous state. Furthermore, the reactions triggered by EB irradiation do not lead to the transformation of the amorphous, thermally conductive ABS/rCF composites into crystalline structures.

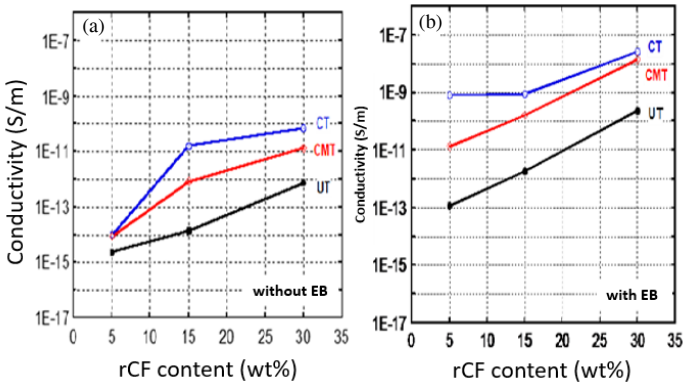

FIGURE 9. Electrical conductivity of differently treated ABS/rCF composites, (a) without EB irradiation and (b) with EB irradiation.

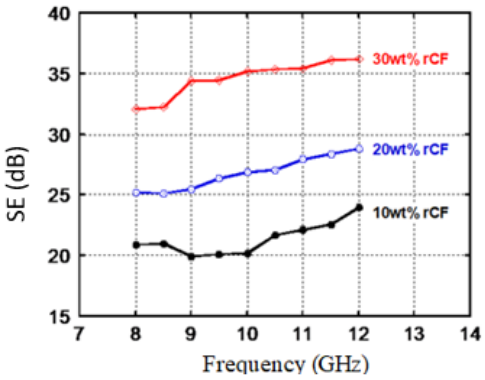

FIGURE 10. Frequency (GHz) dependence of EMI SE rCF/ABS composites containing various amount of rCF.

It is assumed that as the percentage of added ABS amorphous thermoplastic blend increases, the degree of crystallinity of the blend decreases. This observation appears similar to the study conducted by Bhadra and Khastgiris [37]. It is noted that there is a difference in intensity between the XRD patterns of the non-irradiated and irradiated carbon fibre samples at a 30% carbon concentration. This difference suggests that radiation has a positive effect on the surface modification of carbon fibre. The diffraction peaks of the irradiated 70% ABS/30% rCF specimen appeared at $2\theta = 14.1°$, 16.8°, 32.6°, and 36.5°. The deflection peaks for irradiated 30% rCF with 70% ABS samples were observed to be slightly sharpened, as depicted in Figure 8(b). This suggests that the presence of the irradiation dose played a role in the formation of crosslinking networks in the composite, which in turn reduced the gaps between the macromolecular chains and promoted interaction between the ABS chains. As a result, there was a slight increase in the crystallite size of the deflection peak [38]. The presence of a distinct peak in the composite indicates the presence of some degree of crystallinity. However, after irradiation, the intensity of the diffraction peak decreases, and the peak becomes slightly wider, indicating a decrease in crystallinity. Nevertheless, it is worth mentioning that there is no significant alteration in the position of the peak, suggesting that the lattice parameters remain relatively unchanged [39].

3.4. Electrical Conductivity

The transition from mechanical properties to electrical conductivity (Figure 9) and subsequent EMI shielding effectiveness (Figures 10 and 11) establishes a direct logical progression from material modification to functional assessment. Electrical conductivity is the foundational property for conductive EMI shielding materials, as it dictates the material's ability to absorb and reflect electromagnetic waves. Figure 9(a) shows that in non-irradiated samples, conductivity increased with filler content due to conductive path formation, with treated rCF composites consistently outperforming untreated ones. Notably, chemically treated rCF increased conductivity by four orders of magnitude at 25 wt%, though further increase to 30 wt% showed no significant change. Electron beam (EB) irradiation, however, profoundly impacted electrical conductivity, as shown in Figure 9(b). At 200 kGy, EB irradiation significantly enhanced the electrical conductivity of all rCF/ABS composites, particularly for the chemically treated rCF at 30 wt% (2.68×10^{-8} S/m), due to improved rCF dispersion and the formation of a more interconnected conductive network [40].

Chemically-mechanically treated rCF/ABS composites show the highest improvement after EB irradiation, with electrical conductivity increasing from 1.36×10^{-11} to 1.34×10^{-8} (S/m) at 30 wt% rCF content. Irradiated untreated rCF/ABS composites showed a modest increase in electrical conductivity to 2.32×10^{-10} (S/m) at 30 wt% rCF. The lack of increase in electrical conductivity at 30 wt% rCF in the non-irradiated samples can be associated with the agglomeration of rCF in ABS, which hinders percolation and thus decreases the electrical conductivity of the composite. To determine the final electrical properties of ABS composites, the dispersion level of rCF is crucial. Better rCF dispersion levels at 30 weight percent in the composites are attained upon EB irradiation, which results in the creation of an effective network for electron path transmittance and accounts for the increased electrical conductivity found in the irradiated ABS/rCF composites.

3.5. Electromagnetic Interference Shielding Effectiveness of Differently Treated rCF/ABS Composites

Figure 10 displays the shielding effectiveness (SE) results as a function of frequency dependence of EMI SE for rCF/ABS composites containing various amounts of rCF. It has been demonstrated that increasing rCF content, even without irradiation, improves shielding, with a 50% improvement at higher frequencies when rCF is increased from 10% to 30%. This frequency dependency is attributed to the interaction between smaller wavelengths and fiber size [41]. The EMI SE values for both irradiated and non-irradiated rCF-filled ABS composites are displayed in Figure 11. Most crucially, Figure 11(b) illustrates that EB-irradiated samples consistently exhibit superior EMI SE across all composite types compared to their non-irradiated counterparts in Figure 11(a). The irradiated 30 wt% chemically treated rCF/ABS composite achieved an outstanding 46.13 dB in the 8–12 GHz range, representing a 41.5%

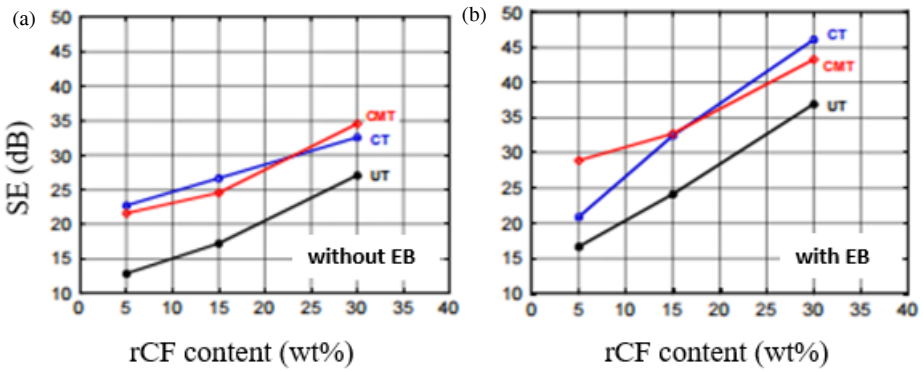

FIGURE 11. EMISE rCF/ABS composites (a) without EB irradiation and (b) with EB irradiation.

improvement. This collective relevance demonstrates how the material modifications (rCF treatment, EB irradiation) synergistically enhance electrical conductivity, which in turn leads to superior EMI shielding performance. The formation of interconnected conductive paths facilitates efficient microwave absorption, reducing both reflection and transmission of incoming radiation. Thus, the mechanical properties ensure the shield's structural integrity, while the tailored electrical properties, refined through irradiation, deliver the core EMI protection functionality, ultimately providing a robust solution for turbulent aerospace environments. The results can be ascribed to the formation of interconnected conductive networks by rCF in the composites because of the EB irradiation. The results of the EB irradiation effect on the SE of ABS/rCF are significant as it has never been examined previously, thus providing technical information necessary for further development of the material as an effective shielding material.

The effect of EB irradiation dosage on the EMI shielding effectiveness of rCF/ABS blends has also been observed. It has been found that EMI SE increases with the increase of EB irradiation dosage. Irradiation promotes the establishment of more interconnected conductive networks resulting from the formation and recombination of free radicals in the polymer-filler interfaces, which facilitates the movement of the mobile charge carriers in the rCF/ABS composites. Conductive fillers interact with the incoming electromagnetic radiation and facilitate the electron transport which is known as microwave absorption across the EMI shielding material by the conductive networks. This is effective in reducing the reflection and transmission of incident radiation. The irradiated ABS composites filled with treated rCF exhibit good electrical conductivity values, which is a determinant factor in a material to behave as an excellent shielding material, to be able to weaken the incident electromagnetic radiation and function as an effective EMI shielding material.

It has also been noted that the effectiveness of rCF/ABS blends' EMI shielding is impacted by the dosage of EB irradiation. It has been discovered that as the dosage of EB irradiation increases, so does EMI SE. Because of the formation and recombination of free radicals in the polymer-filler interfaces, radiation encourages the creation of more interconnected conductive networks, which facilitates the mobility of the mobile charge carriers in the rCF/ABS composites. By interacting with the incoming electromagnetic radiation, the conductive fillers help the conductive networks' conductive networks carry electrons across the EMI shielding material, a process known as microwave absorption. This is effective in reducing incident radiation's reflection and transmission.

3.6. Potential Benefits of Electron Beam Irradiation for EMI Shielding in Turbulent Airplane Environments

Electron beam irradiation offers significant potential for enhancing EMI shielding materials in the demanding environment of turbulent flight. It improves mechanical integrity, crucial for withstanding flight stresses and vibrations, by promoting cross-linking within the polymer matrix (e.g., ABS), increasing strength, toughness, and resistance to fatigue and fracture. This enhanced robustness ensures long-term shielding reliability, preventing structural failures that could compromise its effectiveness. Furthermore, irradiation can improve interfacial bonding between conductive fillers (like carbon fibres) and the matrix, further contributing to the composite's overall mechanical integrity. For specific applications, materials like Teflon (PTFE), known for excellent dielectric properties and chemical inertness, can be incorporated into the broader shielding design [42–44]. Figure 12 shows electron beam irradiation for EMI shielding in turbulent airplane environments. Beyond mechanical enhancements, irradiation directly improves EMI shielding effectiveness. Increased electrical conductivity allows for more efficient attenuation of electromagnetic radiation, protecting sensitive electronics from interference, especially vibration-induced EMI.

The improved conductivity enables more effective absorption and dissipation of electromagnetic energy, minimizing interference with critical avionics. Moreover, irradiation can enhance the uniformity of the conductive network, leading to more consistent shielding performance. Figure 12 shows the example of the electron beam irradiation for EMI shielding in turbulent airplane environments. In cases where Teflon is used for specific components (e.g., high-frequency antenna radomes or cable insulation), its inherent properties, combined with its integration into the overall shielding strategy, contribute to system-wide EMI protection. While Teflon's electrical char-

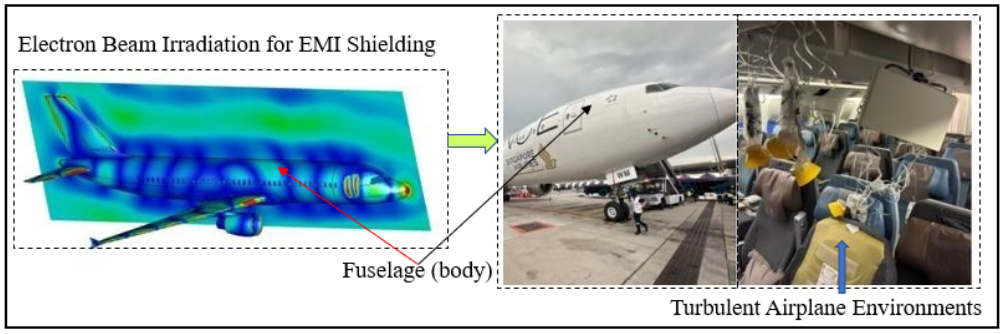

FIGURE 12. Electron beam irradiation for EMI shielding in turbulent airplane environments.

acteristics are advantageous, its mechanical properties can be further enhanced through irradiation, if needed [45–47].

Finally, electron beam irradiation enhances the thermal stability of EMI shielding materials, crucial for maintaining performance in the fluctuating temperatures of flight. Irradiation can improve the material's resistance to thermal degradation, reducing the likelihood of changes in its properties due to temperature variations [48, 49]. This is particularly important in turbulent environments where rapid changes in altitude can lead to significant temperature swings. By improving thermal stability, irradiation ensures that the shielding maintains its effectiveness across a wider range of operating temperatures, contributing to the consistent and reliable protection of electronic systems. Future research will leverage artificial intelligence (AI) and metaheuristic algorithms, such as the grey wolf optimizer (GWO), to optimize the performance of the enhanced EMI shielding rCF/ABS composites. This computational approach, informed by recent advancements in material design [49], aims to develop next-generation composites tailored for high-performance electromagnetic components in applications like 5G, satellite communication, and radar.

The enhanced mechanical and EMI shielding properties of the EB-irradiated rCF/ABS composites make them highly suitable for demanding aerospace applications. These materials could be strategically utilized in various aircraft components where electronics require robust EMI protection without compromising structural integrity or adding significant weight. Specific application areas include avionics bays and electronic enclosures, for protecting sensitive control systems, radar radomes, leveraging the composite's lightweight and EMI shielding capabilities to protect antennas while maintaining signal transparency, and fuselage and wing sections, incorporating the composite into key structural elements for localized EMI shielding of onboard electronics, particularly in areas with high-density wiring and sensor arrays. These components require materials that not only offer high EMI attenuation but also withstand significant mechanical stress and environmental factors, making the composite an ideal candidate.

4. CONCLUSION

CF reclaimed from CF-filled epoxy prepregs can be readily melt-blended with ABS, creating a practical approach for second-generation functional composites for EMI shielding applications. The composites' mechanical properties, including Young's modulus and tensile strength, increased with increasing CF loading, suggesting some degree of interfacial adhesion between the CF and ABS. The electrical conductivity of ABS/rCF composites increases with the amount of rCF, and improvements in both electrical conductivity and shielding effectiveness are also achieved through the rCF treatment. An EB irradiation greatly increases electrical conductivity as well as the effectiveness of EMI shielding, which is likely due to an increase in free radicals from chemical bond breaks. The highest electrical conductivity (1.34×10^{-8} S/m) and EMI SE (46.13 dB) were observed in an irradiated, chemically treated rCF/ABS composite with 30 weight percent rCF content. Overall, this study successfully demonstrated that different treatments, including chemical treatment of rCF and electron beam irradiation, can be used to significantly improve the performance of ABS/rCF composites.

ACKNOWLEDGEMENT

This research was funded by funded by Universiti Teknikal Malaysia Melaka (UTeM) and Dominant Opto's Technologies through Matching Grant No. INDUSTRI(URMG)/DOMINANT/FTKEK/2023/I00084.

REFERENCES

[1] Chung, D. D. L., "Electromagnetic interference shielding effectiveness of carbon materials," *Carbon*, Vol. 39, No. 2, 279–285, 2001.

[2] Tong, X. C., *Advanced Materials and Design for Electromagnetic Interference Shielding*, CRC Press, 2016.

[3] Kashi, S., R. K. Gupta, T. Baum, N. Kao, and S. N. Bhattacharya, "Dielectric properties and electromagnetic interference shielding effectiveness of graphene-based biodegradable nanocomposites," *Materials & Design*, Vol. 109, 68–78, 2016.

[4] Shahzad, F., M. Alhabeb, C. B. Hatter, B. Anasori, S. M. Hong, C. M. Koo, and Y. Gogotsi, "Electromagnetic interference shielding with 2D transition metal carbides (MXenes)," *Science*, Vol. 353, No. 6304, 1137–1140, 2016.

[5] Chen, Z., C. Xu, C. Ma, W. Ren, and H.-M. Cheng, "Lightweight and flexible graphene foam composites for high-performance electromagnetic interference shielding," *Advanced Materials*, Vol. 25, No. 9, 1296–1300, 2013.

[6] Zhang, H., G. Zhang, Q. Gao, M. Zong, M. Wang, and J. Qin, "Electrically electromagnetic interference shielding microcellular composite foams with 3D hierarchical graphene-carbon nanotube hybrids," *Composites Part A: Applied Science and Manufacturing*, Vol. 130, 105773, 2020.

[7] Lei, X., X. Zhang, A. Song, S. Gong, Y. Wang, L. Luo, T. Li, Z. Zhu, and Z. Li, "Investigation of electrical conductivity and electromagnetic interference shielding performance of Au@ CNT/sodium alginate/polydimethylsiloxane flexible composite," *Composites Part A: Applied Science and Manufacturing*, Vol. 130, 105762, 2020.

[8] Geetha, S., K. K. S. Kumar, C. R. K. Rao, M. Vijayan, and D. C. Trivedi, "EMI shielding: Methods and materials — A review," *Journal of Applied Polymer Science*, Vol. 112, No. 4, 2073–2086, 2009.

[9] Jou, W. S., T. L. Wu, S. K. Chiu, and W. H. Cheng, "Electromagnetic shielding of nylon-66 composites applied to laser modules," *Journal of Electronic Materials*, Vol. 30, No. 10, 1287–1293, 2001.

[10] Al-Saleh, M. H. and U. Sundararaj, "Microstructure, electrical, and electromagnetic interference shielding properties of carbon nanotube/acrylonitrile-butadiene-styrene nanocomposites," *Journal of Polymer Science Part B: Polymer Physics*, Vol. 50, No. 19, 1356–1362, 2012.

[11] Li, N., Y. Huang, F. Du, X. He, X. Lin, H. Gao, Y. Ma, F. Li, Y. Chen, and P. C. Eklund, "Electromagnetic interference (EMI) shielding of single-walled carbon nanotube epoxy composites," *Nano Letters*, Vol. 6, No. 6, 1141–1145, 2006.

[12] Yang, Y., M. C. Gupta, K. L. Dudley, and R. W. Lawrence, "Novel carbon nanotube-polystyrene foam composites for electromagnetic interference shielding," *Nano Letters*, Vol. 5, No. 11, 2131–2134, 2005.

[13] Colbert, D. T., "Single-wall nanotubes: A new option for conductive plastics and engineering polymers," *Plastics, Additives and Compounding*, Vol. 5, No. 1, 18–25, 2003.

[14] Eswaraiah, V., V. Sankaranarayanan, and S. Ramaprabhu, "Functionalized graphene-PVDF foam composites for EMI shielding," *Macromolecular Materials and Engineering*, Vol. 296, No. 10, 894–898, 2011.

[15] Kropka, J. M., K. W. Putz, V. Pryamitsyn, V. Ganesan, and P. F. Green, "Origin of dynamical properties in PMMA-C60 nanocomposites," *Macromolecules*, Vol. 40, No. 15, 5424–5432, 2007.

[16] Sichel, E. K., *Carbon Black-polymer Composites: The Physics of Electrically Conducting Composites*, New York Marcel Dekker, Inc., 1982.

[17] Hamed, G. R., "Reinforcement of rubber," *Rubber Chemistry and Technology*, Vol. 73, No. 3, 524–533, 2000.

[18] Adhikari, B., A. K. Ghosh, and S. Maiti, "Developments in carbon black for rubber reinforcement," *Journal of Polymer Materials*, Vol. 17, No. 2, 101–125, 2000.

[19] Hamed, G. R., "Rubber reinforcement and its classification," *Rubber Chemistry and Technology*, Vol. 80, No. 3, 533–544, 2007.

[20] Rahmat, M. and P. Hubert, "Carbon nanotube-polymer interactions in nanocomposites: A review," *Composites Science and Technology*, Vol. 72, No. 1, 72–84, 2011.

[21] Tang, L.-G. and J. L. Kardos, "A review of methods for improving the interfacial adhesion between carbon fiber and polymer matrix," *Polymer Composites*, Vol. 18, No. 1, 100–113, 1997.

[22] Chen, L., K. Zheng, X. Tian, K. Hu, R. Wang, C. Liu, Y. Li, and P. Cui, "Double glass transitions and interfacial immobilized layer in in-situ-synthesized poly (vinyl alcohol)/silica nanocomposites," *Macromolecules*, Vol. 43, No. 2, 1076–1082, 2010.

[23] Chen, M., H. Qu, J. Zhu, Z. Luo, A. Khasanov, A. S. Kucknoor, N. Haldolaarachchige, D. P. Young, S. Wei, and Z. Guo, "Magnetic electrospun fluorescent polyvinylpyrrolidone nanocomposite fibers," *Polymer*, Vol. 53, No. 20, 4501–4511, 2012.

[24] Robertson, C. G. and C. M. Roland, "Glass transition and interfacial segmental dynamics in polymer-particle composites," *Rubber Chemistry and Technology*, Vol. 81, No. 3, 506–522, 2008.

[25] Jouault, N., P. Vallat, F. Dalmas, S. Said, J. Jestin, and F. Boué, "Well-dispersed fractal aggregates as filler in polymer-silica nanocomposites: Long-range effects in rheology," *Macromolecules*, Vol. 42, No. 6, 2031–2040, 2009.

[26] Rittigstein, P., R. D. Priestley, L. J. Broadbelt, and J. M. Torkelson, "Model polymer nanocomposites provide an understanding of confinement effects in real nanocomposites," *Nature Materials*, Vol. 6, No. 4, 278–282, 2007.

[27] Qian, D., W. K. Liu, and R. S. Ruoff, "Load transfer mechanism in carbon nanotube ropes," *Composites Science and Technology*, Vol. 63, No. 11, 1561–1569, 2003.

[28] Yu, M.-F., B. I. Yakobson, and R. S. Ruoff, "Controlled sliding and pullout of nested shells in individual multiwalled carbon nanotubes," *The Journal of Physical Chemistry B*, Vol. 104, No. 37, 8764–8767, 2000.

[29] Qian, D., E. C. Dickey, R. Andrews, and T. Rantell, "Load transfer and deformation mechanisms in carbon nanotube-polystyrene composites," *Applied Physics Letters*, Vol. 76, No. 20, 2868–2870, 2000.

[30] Li, J. and C. L. Cai, "The carbon fiber surface treatment and addition of PA6 on tensile properties of ABS composites," *Current Applied Physics*, Vol. 11, No. 1, 50–54, 2011.

[31] Shin, B. Y. and D. H. Han, "Morphological and mechanical properties of polyamide 6/linear low density polyethylene blend compatibilized by electron-beam initiated mediation process," *Radiation Physics and Chemistry*, Vol. 97, 198–207, 2014.

[32] McNally, T., P. Boyd, C. McClory, D. Bien, I. Moore, B. Millar, J. Davidson, and T. Carroll, "Recycled carbon fiber filled polyethylene composites," *Journal of Applied Polymer Science*, Vol. 107, No. 3, 2015–2021, 2008.

[33] Chen, I., J. K. Hill, R. Ohlemüller, D. B. Roy, and C. D. Thomas, "Rapid range shifts of species associated with high levels of climate warming," *Science*, Vol. 333, No. 6045, 1024–1026, 2011.

[34] Karacan, I. and L. Erzurumluoğlu, "The effect of carbonization temperature on the structure and properties of carbon fibers prepared from poly (m-phenylene isophthalamide) precursor," *Fibers and Polymers*, Vol. 16, No. 8, 1629–1645, 2015.

[35] Bee, S.-T., C. T. Ratnam, L. T. Sin, T.-T. Tee, W.-K. Wong, J.-X. Lee, and A. R. Rahmat, "Effects of electron beam irradiation on the structural properties of polylactic acid/polyethylene blends," *Nuclear Instruments and Methods in Physics Research Section B: Beam Interactions with Materials and Atoms*, Vol. 334, 18–27, 2014.

[36] Hassan, M. M., "Mechanical, thermal, and morphological behavior of the polyamide 6/acrylonitrile-butadiene-styrene blends irradiated with gamma rays," *Polymer Engineering & Science*, Vol. 48, No. 2, 373–380, 2008.

[37] Bhadra, S. and D. Khastgir, "Degradation and stability of polyaniline on exposure to electron beam irradiation (structure-property relationship)," *Polymer Degradation and Stability*, Vol. 92, No. 10, 1824–1832, 2007.

[38] Shah, S., N. L. Singh, A. Qureshi, D. Singh, K. P. Singh, V. Shrinet, and A. Tripathi, "Dielectric and structural modification of proton beam irradiated polymer composite," *Nuclear Instruments and Methods in Physics Research Section B: Beam*

Interactions with Materials and Atoms, Vol. 266, No. 8, 1768–1774, 2008.

[39] Bhadra, S., N. K. Singha, and D. Khastgir, "Dielectric properties and EMI shielding efficiency of polyaniline and ethylene 1-octene based semi-conducting composites," *Current Applied Physics*, Vol. 9, No. 2, 396–403, 2009.

[40] Jia, L.-C., L. Xu, F. Ren, P.-G. Ren, D.-X. Yan, and Z.-M. Li, "Stretchable and durable conductive fabric for ultrahigh performance electromagnetic interference shielding," *Carbon*, Vol. 144, 101–108, 2019.

[41] Lee, J. H., H. Y. Jeong, S. Y. Lee, and S. O. Cho, "Effects of electron beam irradiation on mechanical and thermal shrinkage properties of boehmite/HDPE nanocomposite film," *Nanomaterials*, Vol. 11, No. 3, 777, 2021.

[42] Zeain, M. Y., Z. Zakaria, M. Abu, A. J. A. Al-Gburi, H. Alsariera, A. Toding, S. Alani, M. A. Al-Tarifi, O. S. Al-Heety, H. Lago, and T. Saeidi, "Design of helical antenna for next generation wireless communication," *Przegląd Elektrotechniczny*, Vol. 11, 96–99, 2020.

[43] Zeain, M. Y., M. Abu, Z. Zakaria, A. J. A. Al-Gburi, R. Syahputri, A. Toding, and S. Sriyanto, "Design of a wideband strip helical antenna for 5G applications," *Bulletin of Electrical Engineering and Informatics*, Vol. 9, No. 5, 1958–1963, Oct. 2020.

[44] Cong, L., Z. Guo, X. Zhang, H. Li, H. Jiang, Y. Jing, J. Yan, W. Li, J. Yang, and X. Li, "Effect of electron beam irradiation on the percentage loss of tensile modulus of epoxy polymer," *Polymers*, Vol. 17, No. 4, 447, 2025.

[45] Alsariera, H., Z. Zakaria, A. A. M. Isa, S. Alani, M. Y. Zeain, O. S. Al-Heety, S. Ahmed, M. Mabrok, and R. Alahnomi, "Simple broadband circularly polarized monopole antenna with two asymmetrically connected U-shaped parasitic strips and defective ground plane," *TELKOMNIKA (Telecommunication Computing Electronics and Control)*, Vol. 18, No. 3, 1169–1175, 2020.

[46] Zeain, M. Y., M. Abu, and S. N. Zabri, "Investigation of printed helical antenna using varied materials for ultra-wide band frequency," *Journal of Telecommunication, Electronic and Computer Engineering (JTEC)*, Vol. 10, No. 2-7, 137–142, 2018.

[47] Kurbanova, B., K. Aimaganbetov, K. Ospanov, K. Abdrakhmanov, N. Zhakiyev, B. Rakhadilov, Z. Sagdoldina, and N. Almas, "Effects of electron beam irradiation on mechanical and tribological properties of PEEK," *Polymers*, Vol. 15, No. 6, 1340, 2023.

[48] Alyones, S. and M. Granado, "Extinction efficiency of copper nano fibers in the infrared," *Progress In Electromagnetics Research C*, Vol. 152, 259–262, 2025.

[49] Zeain, M. Y., M. Abu, A. Toding, Z. Zakaria, H. Alsariera, I. Ullah, A. A. Abdulbari, H. Yon, B. S. Taha, and M. I. Abbasi, "Advanced helical antenna design for X-band applications using AI," *Progress In Electromagnetics Research C*, Vol. 153, 201–211, 2025.

[50] Yuan, Y., K. Zhang, Q. Wu, S. N. Burokur, and P. Genevet, "Reaching the efficiency limit of arbitrary polarization transformation with non-orthogonal metasurfaces," *Nature Communications*, Vol. 15, No. 1, 6682, 2024.

[51] Zeain, M. Y., M. Abu, A. A. Althuwayb, H. Alsariera, A. J. A. Al-Gburi, A. A. Abdulbari, and Z. Zakaria, "A new technique of FSS-based novel chair-shaped compact MIMO antenna to enhance the gain for sub-6 GHz 5G applications," *IEEE Access*, Vol. 12, 49 489–49 507, 2024.

[52] Yuan, Y., W. Zhou, H. Zhang, Y. Wang, H. Zong, Y. Wang, Y. Dong, S. N. Burokur, and K. Zhang, "Full-polarimetric synthesized holographic displaying empowered by chirality-assisted metasurface," *Small Science*, Vol. 4, No. 8, 2400138, 2024.

[53] Abd Manaf, M. E., M. I. Shueb, N. Mohamad, N. A. Sani, and A. A. Alkaseh, "Modification of nylon 66/graphene nanoplatelet composites via electron beam irradiation," *Malaysian Journal of Microscopy*, Vol. 18, No. 2, 132–141, 2022.